

# Velocity Curve Analysis of the Spectroscopic Binary Stars NSV 223, AB And, V2082 Cyg, HS Her, V918 Her, BV Dra, BW Dra, V2357 Oph, and YZ Cas by the Non-linear Least Squares

K. Karami<sup>1,2,3,\*</sup>,

R. Mohebi<sup>1,†</sup>,

M. M. Soltanzadeh<sup>1,‡</sup>

<sup>1</sup>Department of Physics, University of Kurdistan, Pasdaran St., Sanandaj, Iran

<sup>2</sup>Research Institute for Astronomy & Astrophysics of Maragha (RIAAM), Maragha, Iran

<sup>3</sup>Institute for Advanced Studies in Basic Sciences (IASBS), Gava Zang, Zanjan, Iran

October 31, 2018

## Abstract

Using measured radial velocity data of nine double lined spectroscopic binary systems NSV 223, AB And, V2082 Cyg, HS Her, V918 Her, BV Dra, BW Dra, V2357 Oph, and YZ Cas, we find corresponding orbital and spectroscopic elements via the method introduced by Karami & Mohebi (2007a) and Karami & Teimoorinia (2007). Our numerical results are in good agreement with those obtained by others using more traditional methods.

Key words. stars: binaries: eclipsing — stars: binaries: spectroscopic

## 1 Introduction

Determining the orbital elements of binary stars helps us to obtain fundamental information, such as the masses and radii of individual stars, that has an important role in understanding the present state and evolution of many interesting stellar objects. Analysis of both light and radial velocity (hereafter RV) curves, derived from photometric and spectroscopic observations, respectively, yields a complete set of basic absolute parameters. One historically well-known method to analyze the RV curve is that of Lehmann-Filhés (cf. Smart, 1990). In the present paper we use the method introduced by Karami & Mohebi (2007a) (=KM2007a) and Karami & Teimoorinia (2007) (=KT2007), to obtain orbital parameters of the nine double-lined spectroscopic binary systems: NSV 223, AB And, V2082 Cyg, HS Her, V918 Her, BV Dra, BW Dra, V2357 Oph, and YZ Cas.

The NSV 223 is a contact system of the A type and the mass ratio is believed to be small (Rucinski et al. 2003a,b). The large semiamplitudes  $K_i$ , suggest that the orbital inclination is close to  $90^\circ$ . The spectral type is  $F7V$  and the period is 0.366128 days (Rucinski et al. 2003a,b). The AB And is a contact binary. The spectral type is  $G8V$ . The period is 0.3318919 days. It is suggested that observed period variability may be a result of the orbital motion

---

\*E-mail: karami@iasbs.ac.ir

†E-mail: rozitamohebi@yahoo.com

‡E-mail: msoltanzadeh@uok.ac.ir

in a wide triple system. The third body should then have to be a white dwarf (Pych et al. 2003,2004). V2082 Cyg is most probably an A-type contact binary with a period of 0.714084 days. The spectral type is *F2V* (Pych et al. 2003,2004). In HS Her, the effective temperatures were found to be  $T_1 = 15200 \pm 750K$  and  $T_2 = 7600 \pm 400K$  for the primary and secondary stars, respectively (Cakirli et al. 2007). The secondary component appears to rotate more slowly. The presence of a third body physically bound to the eclipsing pair has been suggested by many investigators. The two component are located near the zero-age main sequence, with age of about 32 Myr (Cakirli et al. 2007). It is classified as an Algol-type eclipsing binary and single-lined spectroscopic binary. The spectral type of more massive primary component is *B4.5V*. The effective temperature is about  $15200 \pm 750K$  for the primary component and  $7600 \pm 400K$  for the secondary component. The period is 1.6374316 days (Cakirli et al. 2007). The V918 Her is an A-type contact binary. The spectral classification is *A7V*. The period of this binary star is 0.57481 days (Pych et al. 2003,2004). The BV Dra and BW Dra have a circular orbit. From spectrophotometry the components of BV Dra are classified as *F9* and *F8* while the components of BW Dra are *G3* and *G0*. The period of BV Dra is 0.350066 days and for BW Dra is 0.292166 days (Batten & Wenxian 1986). The V2357 Oph was classified as a pulsating star with a period of 0.208 days. The spectral type is *G5V* (Rucinski et al. 2003a,b). The spectral type of primary component of YZ Cas is *A1V* and for the secondary is *F7V*. The period of this binary is 4.4672235 days (Lacy 1981).

This paper is organized as follows. In Sect. 2, we give a brief review of the method of KM2007a and KT2007. In Sect. 3, the numerical results are reported, while the conclusions are given in Section 4.

## 2 A brief review on the method of KM2007a and KT2007

One may show that the radial acceleration scaled by the period is obtained as

$$P\ddot{Z} = \frac{-2\pi K}{(1-e^2)^{3/2}} \sin\left(\cos^{-1}\left(\frac{\dot{Z}}{K} - e \cos \omega\right)\right) \times \left\{1 + e \cos\left(-\omega + \cos^{-1}\left(\frac{\dot{Z}}{K} - e \cos \omega\right)\right)\right\}^2, \quad (1)$$

where the dot denotes the time derivative,  $e$  is the eccentricity,  $\omega$  is the longitude of periastron and  $\dot{Z}$  is the radial velocity of system with respect to the center of mass. Also

$$K = \frac{2\pi}{P} \frac{a \sin i}{\sqrt{1-e^2}}, \quad (2)$$

where  $P$  is the period of motion,  $a$  is the semimajor axis of the orbit and inclination  $i$  is the angle between the line of sight and the normal of the orbital plane.

Equation (1) describes a nonlinear relation,  $P\ddot{Z} = P\ddot{Z}(\dot{Z}, K, e, \omega)$ , in terms of the orbital elements  $K$ ,  $e$  and  $\omega$ . Using the nonlinear regression of Eq. (1), one can estimate the parameters  $K$ ,  $e$  and  $\omega$ , simultaneously. Also one may show that the adopted spectroscopic elements, i.e.  $m_p/m_s$ ,  $m_p \sin^3 i$  and  $m_s \sin^3 i$ , are related to the orbital parameters.

## 3 Numerical Results

Here we use the method of KM2007a and KT2007 to derive both the orbital and combined elements for the nine different double lined spectroscopic systems NSV 223, AB And, V2082

Cyg, HS Her, V918 Her, BV Dra, BW Dra, V2357 Oph, and YZ Cas. Using measured radial velocity data of the two components of these systems obtained by Rucinski et al. (2003a,b) for NSV 223 and V2357 Oph, Pych et al. (2003,2004) for AB And, V2082 Cyg, and V918 Her, Cakirli et al. (2007) for HS Her, Batten & Wenxian (1986) for BV Dra and BW Dra, Lacy (1981) for YZ Cas, the fitted velocity curves are plotted in terms of the photometric phase in Figs. 1 to 9.

Figures 10 to 27 show the radial acceleration scaled by the period versus the radial velocity for the primary and secondary components of NSV 223, AB And, V2082 Cyg, HS Her, V918 Her, BV Dra, BW Dra, V2357 Oph, and YZ Cas, respectively. The solid closed curves are results obtained from the non-linear regression of Eq. (1), which their good coincidence with the measured data yields to derive the optimized parameters  $K$ ,  $e$  and  $\omega$ . The apparent closeness of these curves to ellipses is due to the low, or zero, eccentricities of the corresponding orbits. For a well-defined eccentricity, the acceleration-velocity curve shows a noticeable deviation from a regular ellipse (see Karami & Mohebi 2007b).

The orbital parameters,  $K$ ,  $e$  and  $\omega$ , obtaining from the non-linear least squares of Eq. (1) and the combined spectroscopic elements including  $m_p \sin^3 i$ ,  $m_s \sin^3 i$ ,  $(a_p + a_s) \sin i$  and  $m_p/m_s$  obtaining from the estimated parameters  $K$ ,  $e$  and  $\omega$  for the nine systems are tabulated in Tables 1 to 18, respectively. The velocity of the center of mass,  $V_{\text{cm}}$ , is obtained by calculating the areas above and below of the radial velocity curve. Where these areas become equal to each other, the velocity of center of mass is obtained. Tables 1 to 18 show that the results are in good accordance with the those obtained by Rucinski et al. (2003a,b) for NSV 223 and V2357 Oph, Pych et al. (2003,2004) for AB And, V2082 Cyg, and V918 Her, Cakirli et al. (2007) for HS Her, Batten & Wenxian (1986) for BV Dra and BW Dra, and Lacy (1981) for YZ Cas.

## 4 Conclusions

Using the method introduced by KM2007a and KT2007, we obtain both the orbital elements and the combined spectroscopic parameters of nine double lined spectroscopic binary systems. Our results are in good agreement with the those obtained by others using more traditional methods. In a subsequent paper we intend to study the other different systems.

**Acknowledgements.** This work has been supported financially by Research Institute for Astronomy & Astrophysics of Maragha (RIAAM), Maragha, Iran.

## References

- [1] Batten, A.H., Wenxian, LU.: Pub. Astron. Soc. Pac. **98**, 92 (1986)
- [2] Cakirli, Ö., İbanoğlu, C., Frasca, A.: Astron. Astrophys. **474**, 579 (2007)
- [3] Karami, K., Mohebi, R.: Chin. J. Astron. Astrophys. **7**, 558 (2007a)
- [4] Karami, K., Mohebi, R.: J. Astrophys. Astron. **28**, 217 (2007b)
- [5] Karami, K., Teimoorinia, H.: Astrophys. Space Sci. **311**, 435 (2007)
- [6] Lacy, C.H.: Astrophys. J. **251**, 591 (1981)
- [7] Pych, W., Rucinski, M.S., Debond, H., Thomson, J.R., Capobianco, C.C., Blake, R.M., Ogloza, W., Stachowski, G. Rogoziecki P., & Gazeas K.: astro-ph/0311350 (2003)

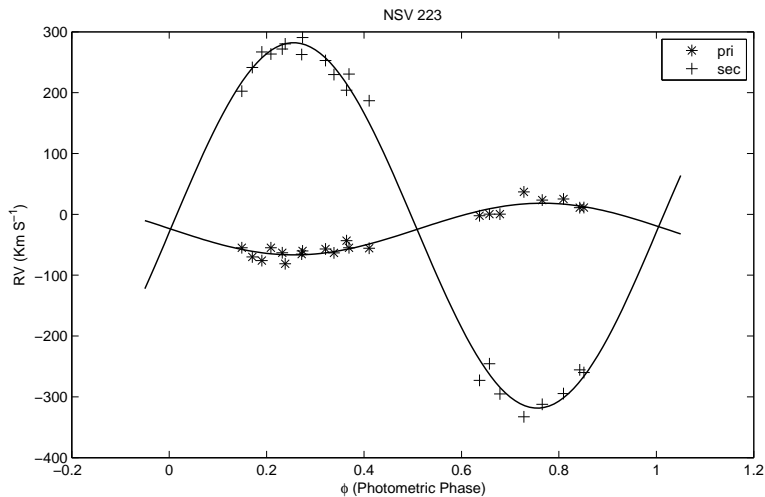


Figure 1: Radial velocities of the primary and secondary components of NSV 223 plotted against the photometric phase. The observational data have been deduced from Rucinski et al. (2003a,b).

- [8] Pych, W., Rucinski, M.S., Debond, H., Thomson, J.R., Capobianco, C.C., Blake, R.M., Ogloza, W., Stachowski, G. Rogoziecki P., & Gazeas, K.: *Astron. J.* **127**, 1712 (2004)
- [9] Rucinski, M.S., Capobianco, C.C., Lu, W., Debond, H., Thomson, J.R., Mochnacki, S.W., Blake, R.M., Ogloza, W., Stachowski, G., Rogoziecki, P.: *astro-ph/0302399* (2003a)
- [10] Rucinski, M.S., Capobianco, C.C., Lu, W., Debond, H., Thomson, J.R., Mochnacki, S.W., Blake, R.M., Ogloza, W., Stachowski, G., Rogoziecki, P.: *Astron. J.* **125**, 3258 (2003b)
- [11] Smart, W.M.: *Textbook on Spherical Astronomy*, 6th edn., Revised by Green, R.M. Cambridge University Press, Cambridge (1990), p.360

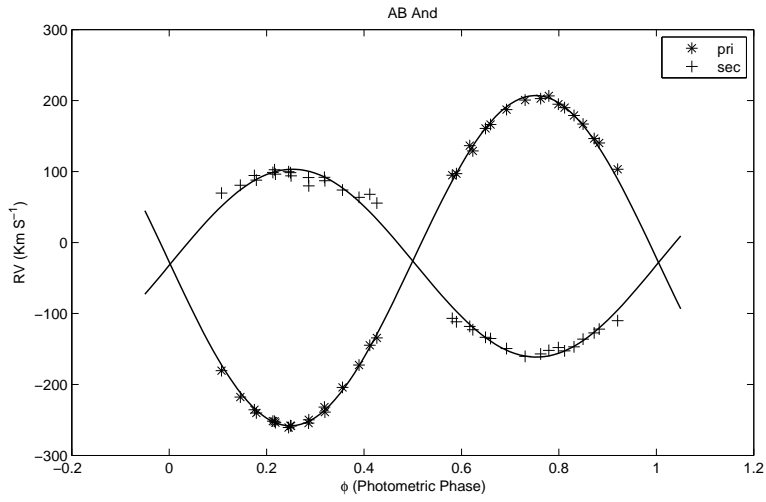


Figure 2: Same as Fig. 1, for AB And. The observational data have been measured by Pych et al. (2003,2004).

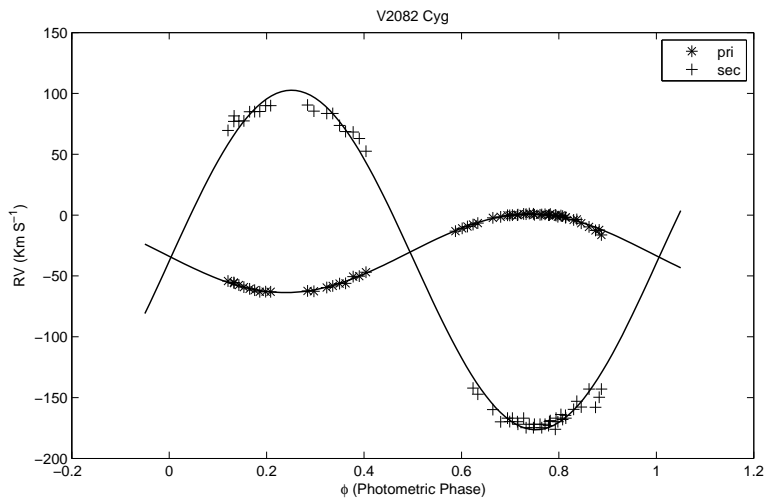


Figure 3: Same as Fig. 1, for V2082 Cyg. The observational data have been derived from Pych et al. (2003,2004).

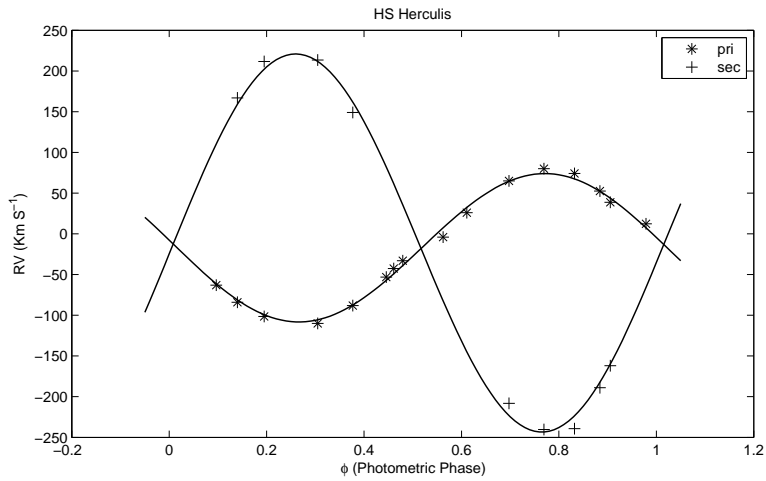


Figure 4: Same as Fig. 1, for HS Her. The observational data are from Cakirli et al. (2007).

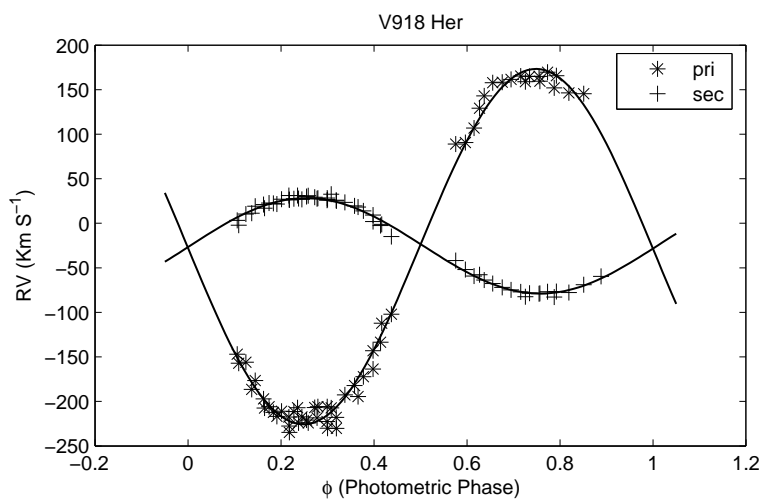


Figure 5: Same as Fig. 1, for V918 Her. The observational data have been derived from Pych et al. (2003,2004).

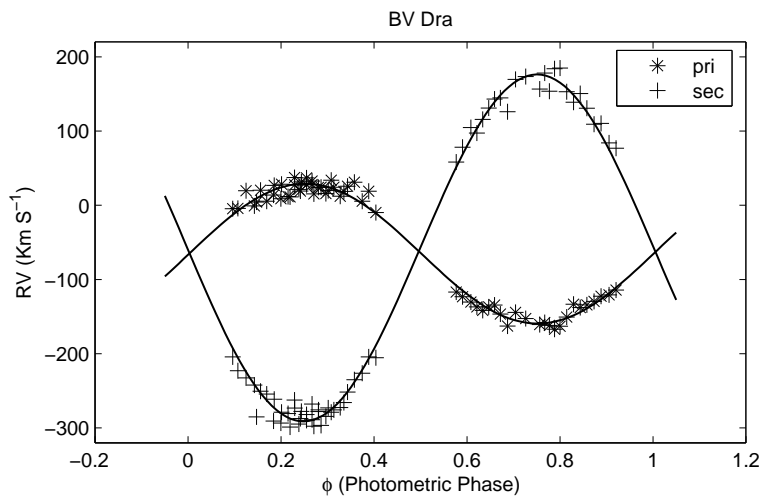


Figure 6: Same as Fig. 1, for BV Dra. The observational data have been derived from Batten & Wenxian (1986).

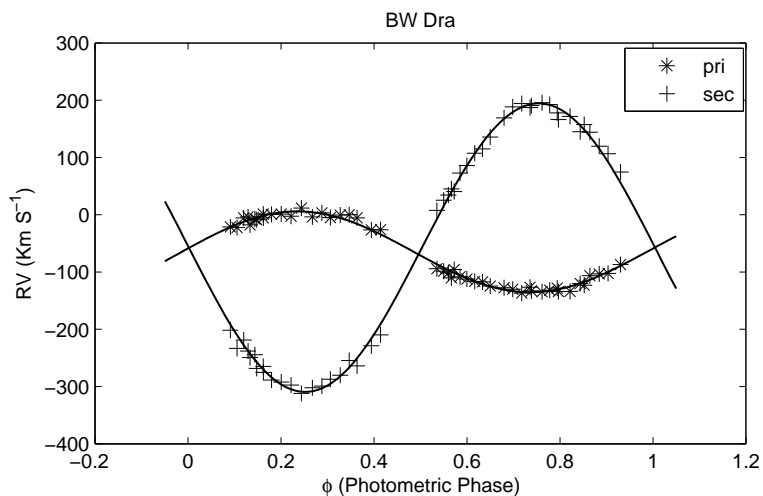


Figure 7: Same as Fig. 1, for BW Dra. The observational data have been derived from Batten & Wenxian (1986).

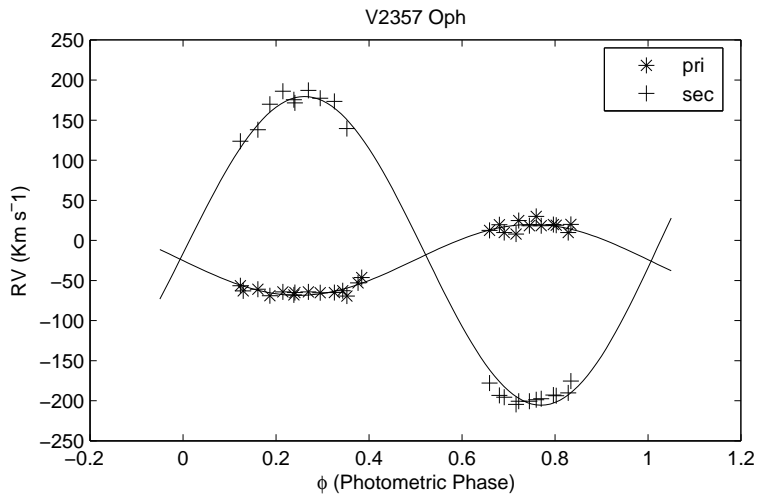


Figure 8: Same as Fig. 1, for V2357 Oph. The observational data have been derived from Rucinski et al. (2003a,b).

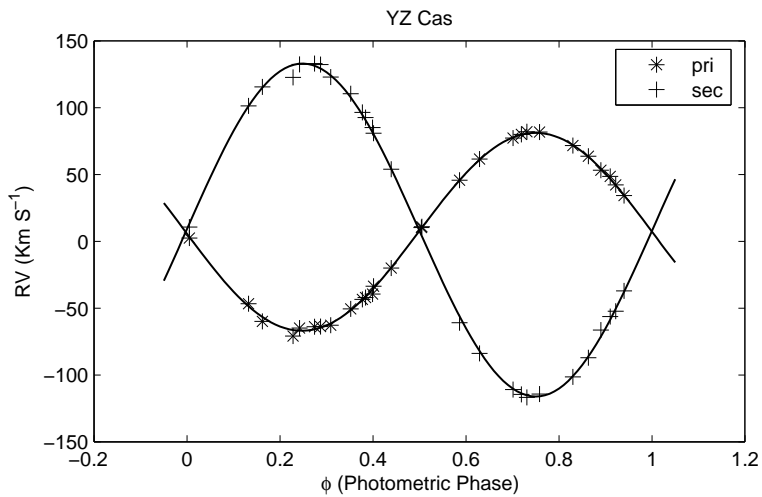


Figure 9: Same as Fig. 1, for YZ Cas. The observational data have been derived from Lacy (1981).



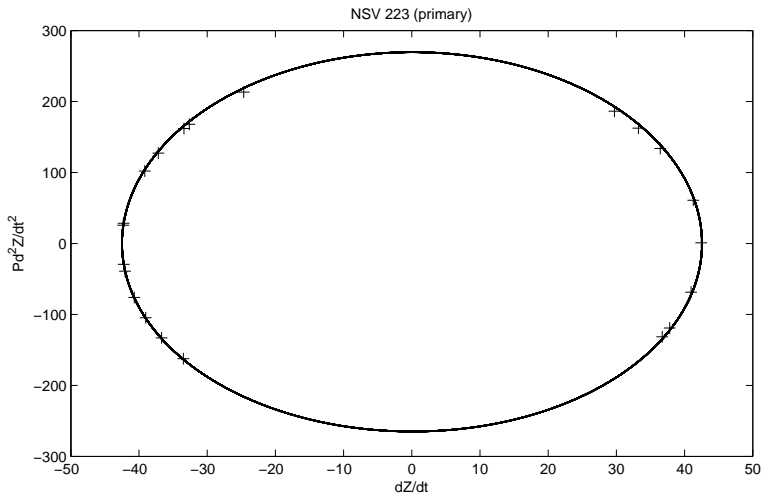


Figure 10: The radial acceleration scaled by the period versus the radial velocity of the primary component of NSV 223. The solid curve is obtained from the non-linear regression of Eq. (1). The plus points are the experimental data.

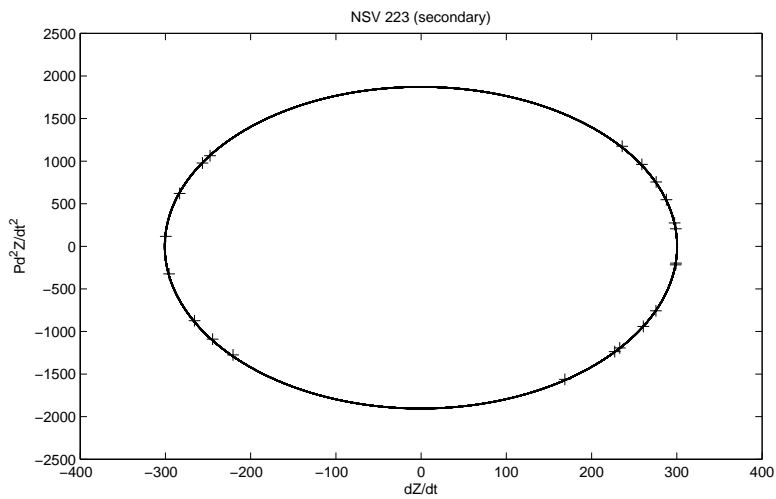


Figure 11: Same as Fig. 10, for the secondary component of NSV 223.

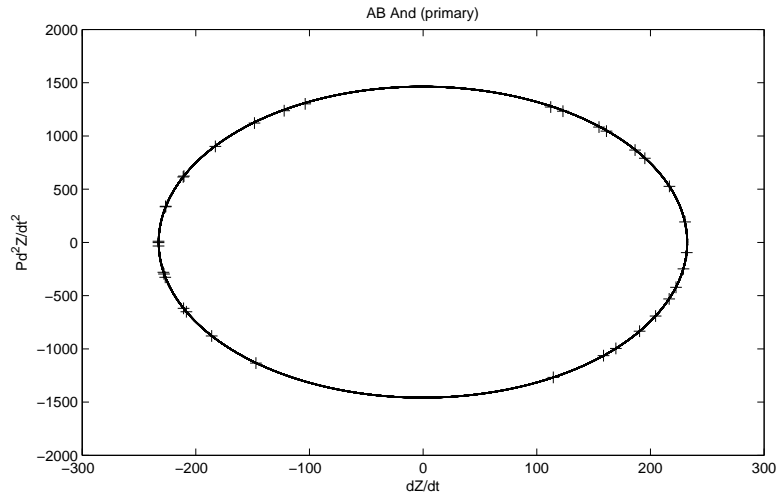


Figure 12: Same as Fig. 10, for the primary component of AB And.

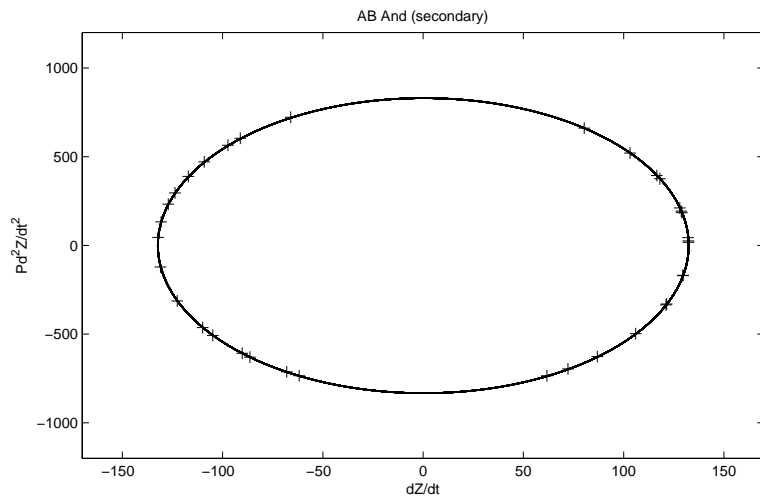


Figure 13: Same as Fig. 10, for the secondary component of AB And.

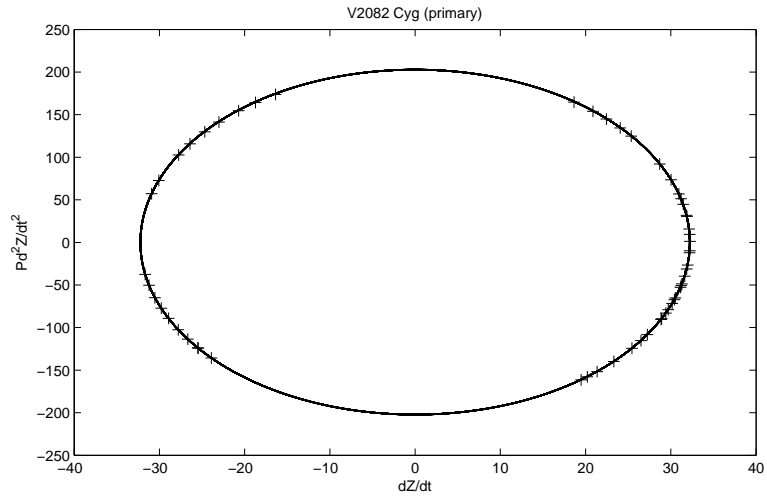


Figure 14: Same as Fig. 10, for the primary component of V2082 Cyg.

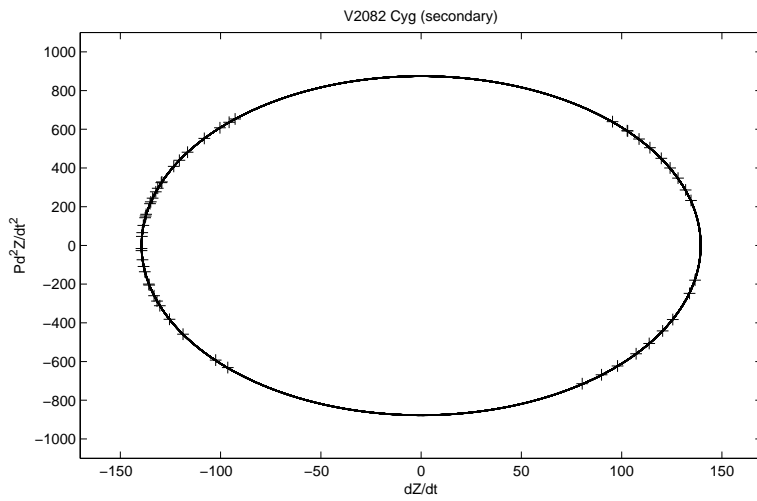


Figure 15: Same as Fig. 10, for the secondary component of V2082 Cyg.

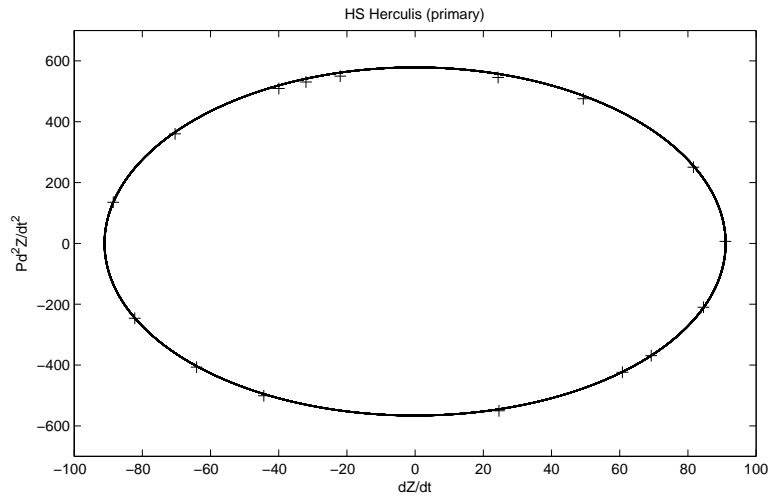


Figure 16: Same as Fig. 10, for the primary component of HS Her.

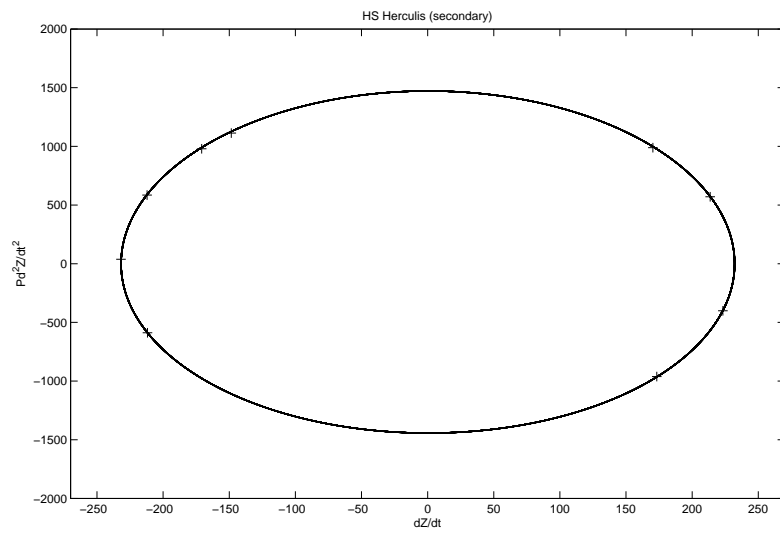


Figure 17: Same as Fig. 10, for the secondary component of HS Her.

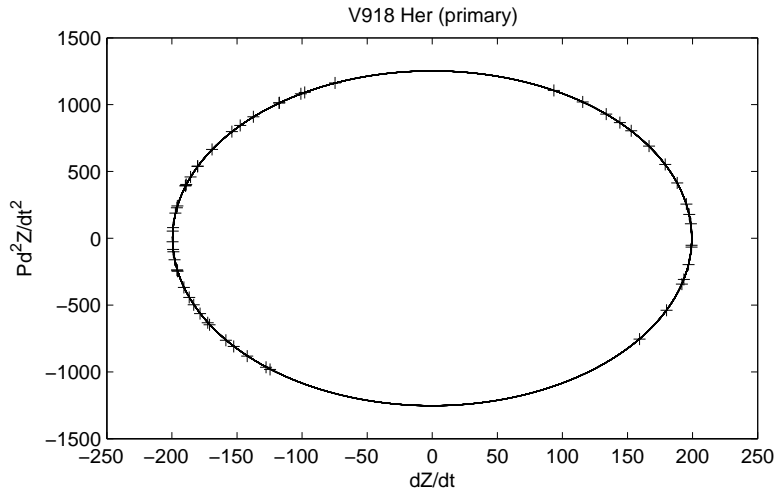


Figure 18: Same as Fig. 10, for the primary component of V918 Her.

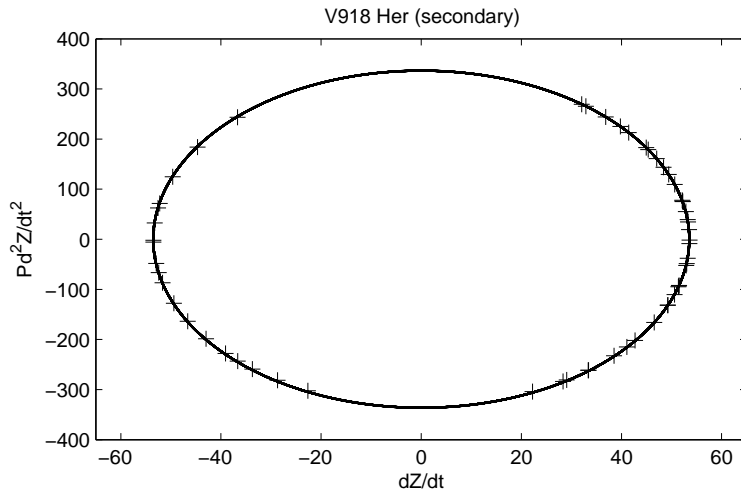


Figure 19: Same as Fig. 10, for the secondary component of V918 Her.

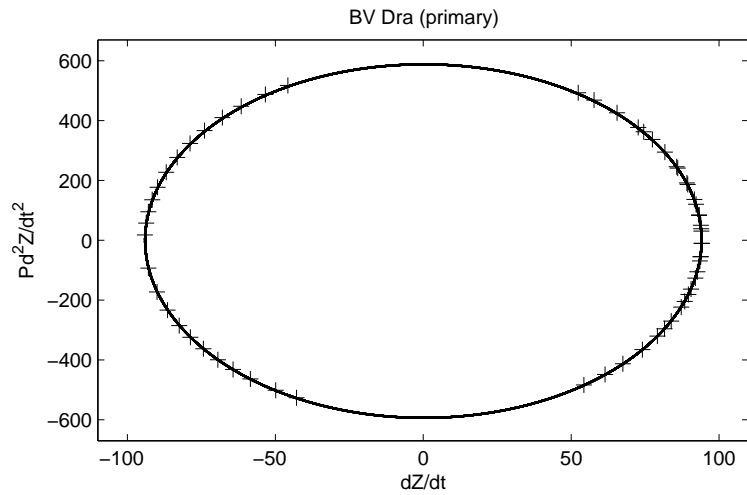


Figure 20: Same as Fig. 10, for the primary component of BV Dra.

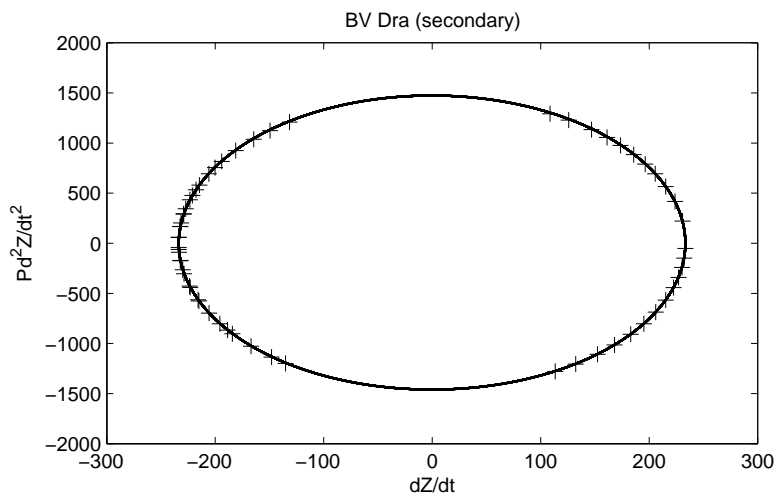


Figure 21: Same as Fig. 10, for the secondary component of BV Dra.

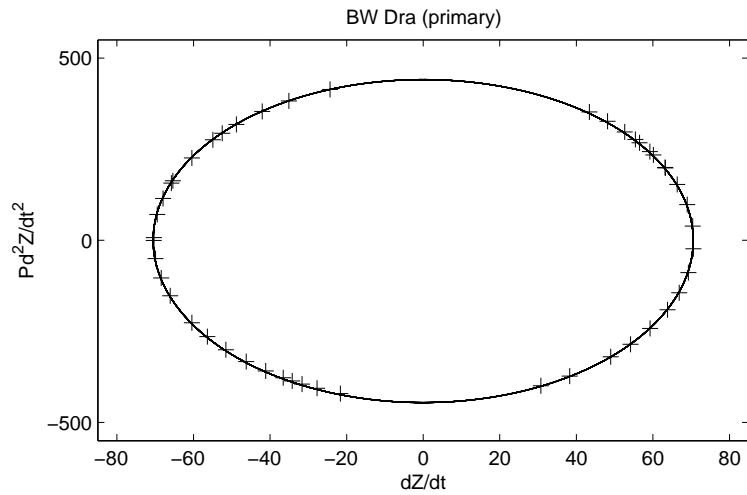


Figure 22: Same as Fig. 10, for the primary component of BW Dra.

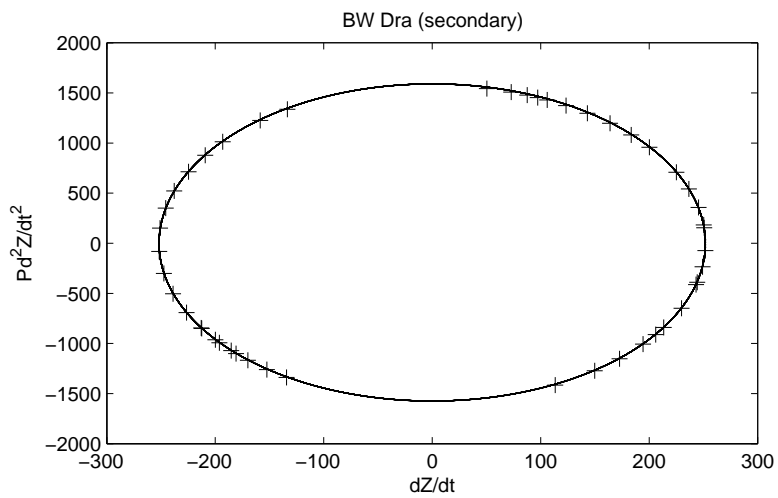


Figure 23: Same as Fig. 10, for the secondary component of BW Dra.

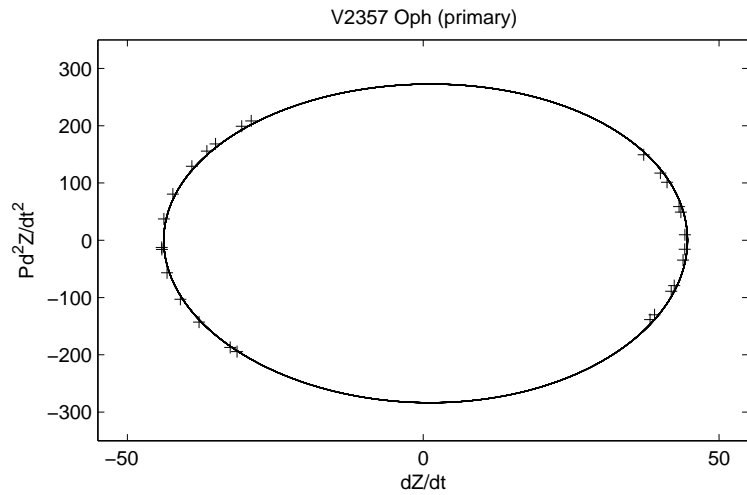


Figure 24: Same as Fig. 10, for the primary component of V2357 Oph.

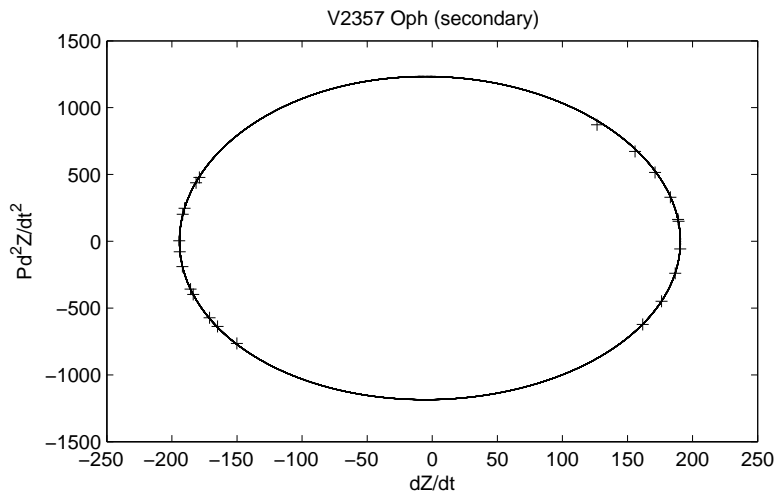


Figure 25: Same as Fig. 10, for the secondary component of V2357 Oph.



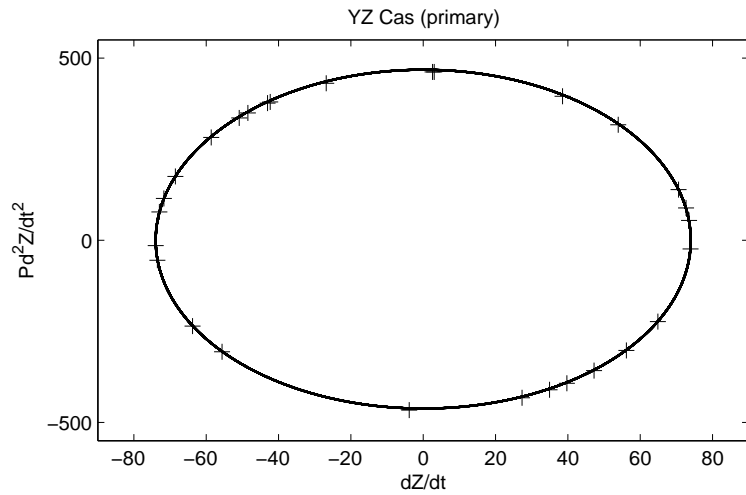


Figure 26: Same as Fig. 10, for the primary component of YZ Cas.

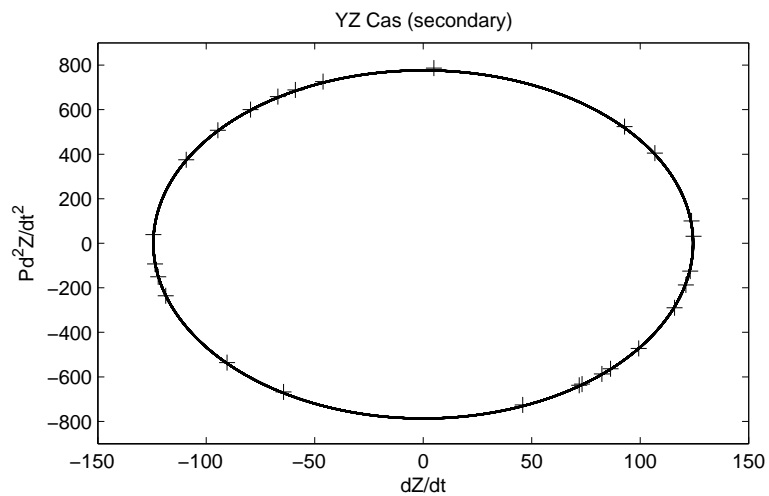


Figure 27: Same as Fig. 10, for the secondary component of YZ Cas.

Table 1: Orbital parameters of NSV 223.

	This Paper	Rucinski et al. (2003a,b)
<b>Primary</b>		
$V_{cm} (kms^{-1})$	$-21.31 \pm 0.98$	$-21.66(2.15)$
$K_p (kms^{-1})$	$42.56 \pm 0.03$	$40.39(2.64)$
$e$	$0.004 \pm 0.001$	—
$\omega(^{\circ})$	$279.40 \pm 12.04$	—
<b>Secondary</b>		
$V_{cm} (kms^{-1})$	$-21.31 \pm 0.98$	$-21.66(2.15)$
$K_s (kms^{-1})$	$300.76 \pm 0.04$	$297.98(4.18)$
$e$	$e_s = e_p$	—
$\omega(^{\circ})$	$\omega_s = \omega_p - 180^{\circ}$	—

Table 2: Spectroscopic elements of NSV 223.

Parameter	This Paper	Rucinski et al. (2003a,b)
$m_p \sin^3 i / M_{\odot}$	$1.3447 \pm 0.0007$	—
$m_s \sin^3 i / M_{\odot}$	$0.1903 \pm 0.0002$	—
$(a_p + a_s) \sin i / R_{\odot}$	$2.4834 \pm 0.0005$	—
$m_s / m_p$	$0.1415 \pm 0.0001$	$0.136(10)$
$(m_p + m_s) \sin^3 i / M_{\odot}$	$1.535 \pm 0.001$	$1.47(9)$

Table 3: Same as Table 1, for AB And

	This Paper	Pych et al. (2003,2004)
<b>Primary</b>		
$V_{cm} (kms^{-1})$	$-27.26 \pm 0.66$	$-27.53(0.67)$
$K_p (kms^{-1})$	$232.69 \pm 0.02$	$232.88(0.83)$
$e$	$0.00109 \pm 0.00005$	—
$\omega(^{\circ})$	$230.69 \pm 3.22$	—
<b>Secondary</b>		
$V_{cm} (kms^{-1})$	$-27.26 \pm 0.66$	$-27.53(0.67)$
$K_s (kms^{-1})$	$132.43 \pm 0.01$	$130.32(1.17)$
$e$	$e_s = e_p$	—
$\omega(^{\circ})$	$\omega_s = \omega_p - 180^{\circ}$	—

Table 4: Same as Table 2, for AB And

Parameter	This Paper	Pych et al. (2003,2004)
$m_p \sin^3 i / M_{\odot}$	$0.6071 \pm 0.0001$	—
$m_s \sin^3 i / M_{\odot}$	$1.0668 \pm 0.0002$	—
$(a_p + a_s) \sin i / R_{\odot}$	$2.3943 \pm 0.0002$	—
$m_p / m_s$	$0.5691 \pm 0.0001$	$0.560(7)$
$(m_p + m_s) \sin^3 i / M_{\odot}$	$1.6739 \pm 0.0004$	$1.648(20)$

Table 5: Same as Table 1, for V2082 Cyg

	This Paper	Pych et al. (2003,2004)
<b>Primary</b>		
$V_{cm} (kms^{-1})$	$-34.19 \pm 0.39$	$-34.12(0.58)$
$K_p (kms^{-1})$	$32.254 \pm 0.003$	$33.16(0.51)$
$e$	$0.0008 \pm 0.0005$	—
$\omega(^{\circ})$	$266.48 \pm 0.06$	—
<b>Secondary</b>		
$V_{cm} (kms^{-1})$	$-34.19 \pm 0.39$	$-34.12(0.58)$
$K_s (kms^{-1})$	$139.50 \pm 0.01$	$139.38(0.99)$
$e$	$e_s = e_p$	—
$\omega(^{\circ})$	$\omega_s = \omega_p - 180^{\circ}$	—

Table 6: Same as Table 2, for V2082 Cyg

Parameter	This Paper	Pych et al. (2003,2004)
$m_p \sin^3 i / M_{\odot}$	$0.3045 \pm 0.0001$	—
$m_s \sin^3 i / M_{\odot}$	$0.07039 \pm 0.00002$	—
$(a_p + a_s) \sin i / R_{\odot}$	$2.4232 \pm 0.0002$	—
$m_s / m_p$	$0.23121 \pm 0.00004$	$0.238(5)$
$(m_p + m_s) \sin^3 i / M_{\odot}$	$0.3749 \pm 0.0001$	$0.380(7)$

Table 7: Same as Table 1, for HS Her

	This paper	Cakirli et al. (2007)
<b>Primary</b>		
$V_{cm} (kms^{-1})$	$-14.24 \pm 0.87$	$-12.8 \pm 1.9$
$K_p (kms^{-1})$	$91.15 \pm 0.02$	$93.4 \pm 2.8$
$e$	$0.048 \pm 0.001$	$0.05 \pm 0.01$
$\omega(^{\circ})$	$268.66 \pm 0.03$	—
<b>Secondary</b>		
$V_{cm} (kms^{-1})$	$-14.24 \pm 0.87$	$-12.8 \pm 1.9$
$K_s (kms^{-1})$	$232.13 \pm 0.01$	$239.4 \pm 3.2$
$e$	$e_s = e_p$	$0.05 \pm 0.01$
$\omega(^{\circ})$	$\omega_s = \omega_p - 180^{\circ}$	—

Table 8: Same as Table 2, for HS Her

Parameter	This study	Cakirli et al. (2007)
$m_p \sin^3 i / M_{\odot}$	$4.116 \pm 0.001$	—
$m_s \sin^3 i / M_{\odot}$	$1.616 \pm 0.001$	—
$(a_p + a_s) \sin i / R_{\odot}$	$10.458 \pm 0.001$	$10.76 \pm 0.50$
$m_s / m_p$	$0.3927 \pm 0.0001$	$0.39 \pm 0.05$

Table 9: Same as Table 1, for V918 Her

	This Paper	Pych et al. (2003,2004)
<b>Primary</b>		
$V_{cm} (kms^{-1})$	$-25.76 \pm 0.78$	$-25.72(0.74)$
$K_p (kms^{-1})$	$199.54 \pm 0.01$	$199.37(1.72)$
$e$	$0.0002 \pm 0.0001$	—
$\omega(^{\circ})$	$315.14 \pm 12.17$	—
<b>Secondary</b>		
$V_{cm} (kms^{-1})$	$-25.76 \pm 0.78$	$-25.72(0.74)$
$K_s (kms^{-1})$	$53.577 \pm 0.001$	$53.93(0.49)$
$e$	$e_s = e_p$	—
$\omega(^{\circ})$	$\omega_s = \omega_p - 180^{\circ}$	—

Table 10: Same as Table 2, for V918 Her

Parameter	This Paper	Pych et al. (2003,2004)
$m_p \sin^3 i / M_{\odot}$	$0.20442 \pm 0.00002$	—
$m_s \sin^3 i / M_{\odot}$	$0.7613 \pm 0.0001$	—
$m_p / m_s$	$0.26851 \pm 0.00001$	$0.271(5)$
$(m_p + m_s) \sin^3 i / M_{\odot}$	$0.9657 \pm 0.0001$	$0.968(21)$

Table 11: Same as Table 1, for BV Dra

	This Paper	Batten & Wenxian (1986)
<b>Primary</b>		
$V_{cm} (kms^{-1})$	$-61.23 \pm 0.77$	$-65.2 \pm 1.2$
$K_p (kms^{-1})$	$94.119 \pm 0.002$	$93.9 \pm 1.4$
$e$	$0.0025 \pm 0.0003$	—
$\omega(^{\circ})$	$256.06 \pm 11.18$	—
<b>Secondary</b>		
$V_{cm} (kms^{-1})$	$-61.23 \pm 0.77$	$-57.7 \pm 1.7$
$K_s (kms^{-1})$	$139.50 \pm 0.01$	$139.38(0.99)$
$e$	$e_s = e_p$	—
$\omega(^{\circ})$	$\omega_s = \omega_p - 180^{\circ}$	—

Table 12: Same as Table 2, for BV Dra

Parameter	This Paper	Batten & Wenxian (1986)
$a_p \sin i / 10^6$	$0.453 \pm 0.001$	$0.452 \pm 0.007$
$a_s \sin i / 10^6$	$1.1248 \pm 0.0001$	$1.124 \pm 0.010$
$m_p \sin^3 i / M_{\odot}$	$0.9106 \pm 0.0002$	$0.911 \pm .020$
$m_s \sin^3 i / M_{\odot}$	$0.36679 \pm 0.00006$	$0.366 \pm 0.010$
$m_s / m_p$	$0.40278 \pm 0.00004$	$0.402 \pm 0.007$

Table 13: Same as Table 1, for BW Dra

	This Paper	Batten & Wenxian (1986)
<b>Primary</b>		
$V_{cm} (kms^{-1})$	$-61.14 \pm 0.73$	$-64.2 \pm 0.9$
$K_p (kms^{-1})$	$70.59 \pm 0.03$	$70.5 \pm 1.1$
$e$	$e_p = e_s$	—
$\omega(^{\circ})$	$270.58 \pm 0.44$	—
<b>Secondary</b>		
$V_{cm} (kms^{-1})$	$-61.14 \pm 0.73$	$-57.4 \pm 1.4$
$K_s (kms^{-1})$	$252.018 \pm 0.005$	$251.5 \pm 1.7$
$e$	$0.0026 \pm 0.0001$	—
$\omega(^{\circ})$	$\omega_s = \omega_p - 180^{\circ}$	—

Table 14: Same as Table 2, for BW Dra

Parameter	This Paper	Batten & Wenxian (1986)
$a_p \sin i / 10^6$	$0.2836 \pm 0.0001$	$0.283 \pm 0.004$
$a_s \sin i / 10^6$	$1.01249 \pm 0.00002$	$1.010 \pm 0.007$
$m_p \sin^3 i / M_{\odot}$	$0.7939 \pm 0.0001$	$0.791 \pm 0.015$
$m_s \sin^3 i / M_{\odot}$	$0.2224 \pm 0.0001$	$0.222 \pm 0.005$
$m_p / m_s$	$0.2801 \pm 0.0001$	$0.280 \pm 0.005$

Table 15: Orbital parameters of V2357 Oph.

	This Paper	Rucinski et al. (2003a,b)
<b>Primary</b>		
$V_{cm} (kms^{-1})$	$-17.79 \pm 0.63$	$-19.12(1.64)$
$K_p (kms^{-1})$	$44.29 \pm 0.07$	$44.12(1.63)$
$e$	$e_p = e_s$	—
$\omega(^{\circ})$	$227.12 \pm 0.23$	—
<b>Secondary</b>		
$V_{cm} (kms^{-1})$	$-17.79 \pm 0.63$	$-19.12(1.64)$
$K_s (kms^{-1})$	$192.52 \pm 0.02$	$190.93(2.90)$
$e$	$0.0134 \pm 0.0004$	—
$\omega(^{\circ})$	$\omega_s = \omega_p - 180^{\circ}$	—

Table 16: Spectroscopic elements of V2357 Oph.

Parameter	This Paper	Rucinski et al. (2003a,b)
$m_p \sin^3 i / M_{\odot}$	$0.4647 \pm 0.0004$	—
$m_s \sin^3 i / M_{\odot}$	$0.1069 \pm 0.0002$	—
$m_s / m_p$	$0.2300 \pm 0.0004$	$0.231(10)$
$(m_p + m_s) \sin^3 i / M_{\odot}$	$0.5716 \pm 0.0007$	$0.560(32)$

Table 17: Same as Table 1, for YZ Cas

	This Paper	Lacy (1981)
<b>Primary</b>		
$V_{cm} (kms^{-1})$	$7.78 \pm 0.58$	$8.14 \pm 0.06$
$K_p (kms^{-1})$	$74.039 \pm 0.002$	$73.35 \pm 0.21$
$e$	$0.0034 \pm 0.0001$	$0.0 \pm 0.003$
$\omega(^{\circ})$	$270.078 \pm 0.395$	—
<b>Secondary</b>		
$V_{cm} (kms^{-1})$	$7.78 \pm 0.58$	$8.14 \pm 0.06$
$K_s (kms^{-1})$	$124.49 \pm 0.05$	$125.7 \pm 0.5$
$e$	$e_s = e_p$	—
$\omega(^{\circ})$	$\omega_s = \omega_p - 180^{\circ}$	—

Table 18: Same as Table 2, for YZ Cas

Parameter	This Paper	Lacy (1981)
$a_p \sin i / 10^6$	$4.548 \pm 0.003$	$4.508 \pm 0.012$
$a_s \sin i / 10^6$	$7.6470 \pm 0.0001$	$7.727 \pm 0.031$
$m_p / M_{\odot}$	$2.274 \pm 0.002$	$2.31 \pm 0.01$
$m_s / M_{\odot}$	$1.352 \pm 0.001$	$1.35 \pm 0.02$